



# Global dataset of storm surges and extreme sea levels for 1950-2024 based on the ERA5 climate reanalysis

Natalia Aleksandrova<sup>1</sup>, Jelmer Veenstra<sup>1</sup>, Sanne Muis<sup>1,2</sup>

<sup>1</sup>Department of Hydrodynamics and Forecasting, Deltares, Delft, 2629 HV, The Netherlands

<sup>2</sup>Department of Water and Climate Risk, Faculty of Science, Vrije Universiteit Amsterdam, Amsterdam, 1081 HV, The Netherlands

*Correspondence to:* Natalia Aleksandrova (natalia.aleksandrova@deltares.nl)

**Abstract.** Extreme sea levels, generated by storm surges and high tides, can cause coastal flooding and erosion. Global datasets have been instrumental in mapping extreme sea levels and associated societal risks. Harnessing the backward extension of the ERA5 reanalysis, we present a dataset containing timeseries of tides and storm surges based on a global hydrodynamic model covering the period 1950-2024. This is an extension of a previously published dataset that covered a shorter period (1979-2018). Using this dataset, we estimate extreme sea levels globally. Validation shows good agreement between observed and modelled extreme sea levels, with the level of agreement for the extended dataset being very similar to that of the previously published dataset. The extended 75-year dataset allows for a more robust estimation of return periods, often resulting in smaller uncertainties than its 40-year precursor. This underscores the necessity for long timeseries and the strength of long-term modelling enabled by the ERA5 reanalysis extension. The present dataset can be used for assessing flood risk, climate variability and climate changes.

## 1 Introduction

Extreme sea levels, driven by the combination of mean sea level, tides, storm surges and waves (Woodworth et al., 2019), can drive coastal flooding. Global reanalysis of extreme sea levels that have improved our understanding of the driving mechanisms of coastal flooding at large-scales (Hinkel et al., 2021). The reanalysis datasets have been used to estimate exceedance probabilities, which are valuable input for coastal flood risk assessment that are used for both disaster risks reductions and climate change mitigation and adaptation (Tiggelhoven et al., 2020). One of the first global reanalysis dataset of still sea levels, called the Global Tide and Surge Reanalysis (GTSR) dataset was published in 2016 (Muis et al., 2016). This dataset was based on surge simulations of Global Tide and Surge Model version 2.0 (GTSMv2.0) forced with ERA-Interim, which were superimposed with tide simulations of the FES2012 model (Carrere et al., 2012). The hydrodynamic approach has a higher accuracy than previous global return periods of extreme sea levels that used simple linear approximations (Muis et al., 2017; Hinkel et al., 2014). Moreover, a modelling approach provides an improved spatial coverage compared to previous quasi global assessment that were based on sparse dataset of observations (Menéndez and Woodworth, 2010; Fang et al., 2014). In 2020, an updated reanalysis dataset was published based on GTSMv3.0 forced with



the ERA5 climate reanalysis (Muis et al., 2020). Model development allowed to include tides from the same model, and thereby account for non-linear interaction between tides and storm surge which has shown to be important in shallow regions with a large tidal range (Arns et al., 2020). The ERA5 reanalysis has a much higher spatial and temporal resolution than its predecessor ERA-Interim (31 vs. 78 km; 1 hour vs. 6 hours). This has greatly improved the performance of global surge  
 35 modelling, particularly in regions prone to tropical cyclones (Muis et al., 2020; Dullaart et al., 2020).

The GTSM-derived timeseries of still water levels can be used to analyse individual historical events both in terms of the height of water levels (Dullaart et al., 2020) and their impact (Koks et al., 2023). The dataset is also used to investigate the event footprint and spatial dependencies (Enriquez et al., 2020; Li et al., 2023), as well as the influence of climate variability  
 40 and climate change on surge levels (Muis et al., 2018; Muis et al., 2023a). A recent assessment on the drivers of shoreline changes of the global coastline shows that despite clear changes in storm surges, there is no clear link with shoreline changes (Ghanavati et al., 2023). The GTSM-ERA5 reanalysis has also been used to remove the meteorological influence from the historical observed sea-level trends for the Dutch coast, which helped to reveal an acceleration of the sea-level rise (Stolte et al., 2023). The dataset has also been used to assess the dependency between storm surge and other flood drivers (Couasnon  
 45 et al., 2020; Ridder et al., 2020; Nasr et al., 2021; Camus et al., 2021) and its influence on (compound) flooding (Couasnon et al., 2020; Ikeuchi et al., 2017; Eilander et al., 2020). Since GTSM is a barotropic depth-averaged model, some coastal processes are not well-captured. Several studies have improved this by supplementing the reanalysis with other data. This includes combining the return periods of still water levels with estimates of wave setup based on the significant wave height from ERA5 (Kirezci et al., 2020) and with mean sea levels from ocean reanalysis to better capture the mean sea level  
 50 response (Muis et al., 2018; Treu et al., 2023).

The timeseries of water levels are used to derive statistical parameters, such as percentiles and return periods. Different methods, such as annual maxima and peaks-over-threshold have been applied. The return periods have been used in a wide range of studies and form the basis of many large-scale assessments of coastal flood hazard and risk (Tiggelhoven et al.,  
 55 2020; Lincke and Hinkel, 2018; Brown et al., 2018), including infrastructure and cultural heritage sites (Reimann et al., 2018; Verschuur et al., 2023).

The current GTSM-ERA5 reanalysis dataset covers the period 1979 to 2018. The length of 40 years is relatively short considering the large decadal variability (Calafat et al., 2022) and the large uncertainties associated with fitting an extreme  
 60 value distribution (Wahl et al., 2017). Recently, the ERA5 climate reanalysis was extended backwards to 1940 (Bell et al., 2021; Hersbach et al., 2023), seamlessly joining with the dataset covering 1979 to the present. The quality of the reanalysis was improved by assimilating additional conventional observations, as well as through making better use of early satellite data. While trend analysis before the satellite-era should be carefully done (Tadesse et al., 2022), the ERA5 dataset extension



allows to also extend the storm surge reanalysis dataset derived using GTSM. Such an extended dataset may reduce the  
65 uncertainty of the extreme values fit and would allow to quantify decadal variability more accurately.

In this paper, we present an extension of the previous surge reanalysis dataset published in 2020 that covered the period  
1979-2018 (Muis et al., 2020). We use the same modelling chain, which consists of GTSMv3.0 in combination with tidal and  
meteorological forcing as well as annual mean sea level. Leveraging the backward extension of ERA5 dataset, we extend the  
70 surge sea level dataset to span a period from 1950 to 2024, resulting in the GTSM-ERA5-E dataset. To achieve this, a  
portable and easily repeatable workflow was developed, that can be used to deploy Global Tide and Surge Model (GTSM)  
on a high-performance computing (HPC) cluster. We describe the workflow that was used to produce the dataset, validate  
the dataset against observed sea levels, and we show the effect of longer records on the extreme value analysis and  
associated uncertainties.

## 75 2 Methodology

The workflow consists of three main steps that are visualized in Figure 1. The first step is the *model simulations* (blue  
colours in Figure 1), which consists of pre-processing input data, running GTSM, and post-processing of output data into  
timeseries per geographical location. The second step is the *analysis* of the timeseries data on a global scale using extreme  
value statistics (yellow colours in Figure 1). The third step is the *validation* of the modelled water levels against observed  
80 water levels at selected stations (green colours in Figure 1).

The workflow is realized through a combination of Python and bash scripts. All the simulations are run on the Dutch  
National Supercomputer Snellius, which makes use of SLURM job scheduler. Each step of the workflow is semi-automated  
where the bash scripts are used to submit specific jobs. The data processing and analysis are largely done with Python 3  
85 using the *xarray* package (Hoyer and Hamman, 2017), whereas the model simulations make use of the Delft3D Flexible  
Mesh software (Kernkamp et al., 2011).

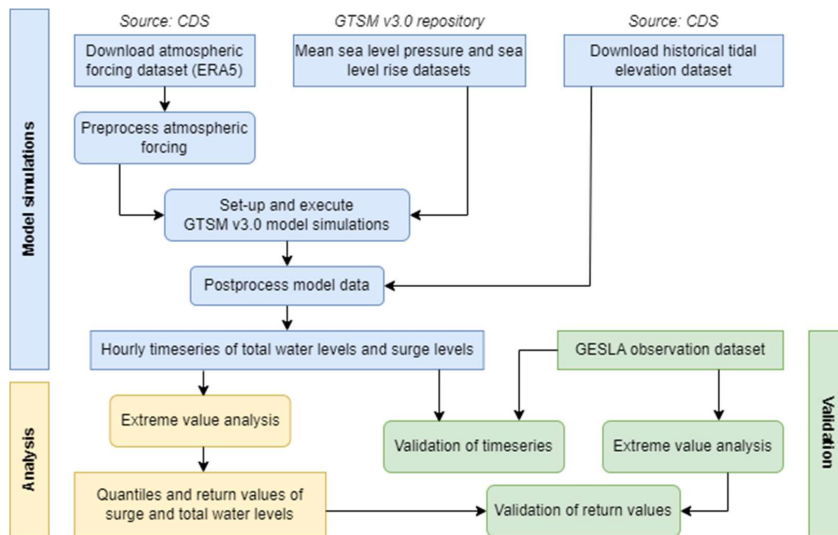


Figure 1: Flow chart of the main workflow that was used to generate the GTSM-ERA5-E water level reanalysis.

90

## 2.1 Model simulations

We use the recent backward extension of the ERA5 climate reanalysis (Hersbach et al., 2023) to simulate time series of still water levels from 1950 to 2024. Hourly wind speed and atmospheric pressure ( $u_{10}$ ,  $v_{10}$ , and  $msl$ ) are downloaded from the Climate Data Store (CDS) by Copernicus Climate Change Service (C3S). In a preprocessing step, we adjust the format of the meteorological data to make it compatible with the hydrodynamic modelling software. Sea level rise is included in the simulations by using a spatially-varying dataset of annual mean sea levels (Muis et al., 2023b). The underlying sea level rise data was compiled using the probabilistic model of Le Bars (2018) and is defined at a spatial resolution of  $1^\circ \times 1^\circ$ ; the data for 1950-2016 is based on observations, and the data from 2016 onwards is based on projections from the mean ensemble Fifth Assessment Report (AR5) of the Intergovernmental Panel on Climate Change (IPCC, 2013). The detailed methodology behind the sea level rise dataset is provided in the supporting information for the previous publication where this dataset was utilized (Muis et al., 2020). After the model is initialized, the pressure and wind speed forcing from ERA5 is applied, and to harmonize the vertical reference of the water levels the yearly mean sea level pressure over 1986-2005 is subtracted via an additional correction in the form of a negative pressure field (Muis et al., 2023b).

We simulate tides and storm surges with GTSMv3.0 using the same configuration as described in previous work (Muis et al., 2020). The GTSMv3.0 is a depth-averaged hydrodynamic model with global coverage that dynamically simulates tides and



storm surges. GTSMv3.0 is based on the unstructured Delft3D Flexible Mesh software (Kernkamp et al., 2011). We make use of a singularity container, which allows us to run Delft3D Flexible Mesh on any HPC cluster in a simple, portable, and reproducible way. GTSM has a spatially varying resolution, which goes up to 2.5 km at the global coast and 1.25 km at the European coast. The bathymetry is derived from various sources: General Bathymetric Chart of the Ocean (GEBCO) with a 30 arc seconds resolution (GEBCO, 2014), European Marine Observation and Data Network (EMODnet) at 250 m resolution in Europe (EMODnet Bathymetry Consortium, 2018), and Bedmap2 for the bathymetry under and thickness of the permanent ice shelves in Antarctica (Fretwell et al., 2013). These datasets are internationally recognized, openly available, and provide full global coverage. However, it must be noted that the GEBCO dataset has a relatively low resolution and can carry significant uncertainty in data-scarce regions. This limitation is inherent to the global modelling based on open data. The model has no open boundaries. Tides are induced by including tide generating forces using a set of 60 frequencies (tidal constituents), defined in Delft3D Flexible Mesh software and selected to achieve optimal trade-off between accuracy and computational efficiency. Storm surges are generated by the transfer of momentum from the wind to the water, with an additional contribution by the changes in atmospheric pressure through the inverse barometer effect. We use the Charnock formulation (Charnock, 1955) with a drag coefficient of 0.041 to estimate the wind stress at the ocean surface. To minimize the data storage requirements, we use a set of 44,734 output locations (Muis et al., 2020) that include ~18,000 coastal points every ~10-50 km along the coast and ocean points on a semiregular grid at a resolution that varies between 0.25° and 5°. The model runs are set up using an automatized workflow by creating separate yearly model simulations with a spin-up time of 15 days, and a timestep of 10 minutes. Using a parallel setup with 128 cores and 224 GB of RAM, each 1-year simulation takes approximately 1 day to complete. Subsequently the output from the yearly simulations can be combined to obtain the full dataset by removing the spin-up part of the simulation.

In the postprocessing step we compute storm surge levels as a difference between a total water level simulation and a tide-only simulation. For this we use a tide-only simulation that is already available from CDS and covers the same period (Muis et al., 2025a). In addition, the NetCDF4 file format is optimized, the data for the spin-up period is removed, unnecessary variables are dropped, and metadata is prescribed. Datasets with timeseries of hourly mean water levels and daily maximum water levels are derived directly from the 10-minute timeseries of water levels.

## 2.2 Data analysis

The data analysis consists of three steps. First, we detrend the timeseries by removing the annual means. Second, we compute various descriptive statistics at each output location, such as mean, minima, maxima, standard deviation and percentiles. Third, we apply extreme value analysis (EVA) to estimate the exceedance probabilities of the still water levels. Following Wahl et al. (2017), we apply the Peak Over Threshold (POT) approach and we fit the Generalized Pareto Distribution (GPD) on the peaks that exceed the 99th percentile water level, then we derive estimates for various return periods, including confidence intervals. We use a 72-hour window for the de-clustering of the events to ensure their



140 independence. We use the Maximum Likelihood Estimation (MLE) to fit the GPD parameters. This analysis is realized using  
 the *pyextremes* package (Bocharov, 2023). The analysis is done for the extended period (1950-2024), as well as the original  
 period (1979-2018) to enable comparison between datasets of different duration.

### 2.3 Validation

To validate the dataset, we compare the modelled still water levels with high-frequency observations of sea levels from the  
 145 tide gauge stations in the Global Extreme Sea Level Analysis (GESLA) dataset, version 3 (Haigh et al., 2022). We only use  
 the tide gauge stations where the available observations span a period of at least 50 years overlapping with the period  
 covered by ERA5 (1950-2024), and where no more than 25% of data is missing from that period. Additionally, the data  
 records are filtered according to the data quality flag value to only use records where no data quality issues are indicated.  
 This selection results in 262 stations that can be used for extreme value analysis, where each station has a counterpart  
 150 location in the GTSM-ERA5-E dataset (located less than 10km away). The data coverage in the resulting observational  
 dataset used for data validation is 84% (on average across stations) in the period of 1950-2024, with a higher coverage of  
 95% in the period 1979-2018.

Each observation record is resampled to hourly data and detrended by removing the annual mean sea level. Next, we  
 155 calculate percentiles and estimate the extreme sea levels using extreme value analysis based on this data, using the same  
 methodology as for the GTSM-derived sea levels.

The model performance of GTSM-ERA5-E is evaluated by comparing observed and modelled values for various percentiles  
 and return periods. For each station, the model data is filtered to only include the periods where observation data is available,  
 160 this is done before calculating the statistical parameters for comparison. We use the mean bias (MB), the mean absolute error  
 (MAE), and the mean absolute percentage error (MAPE) to compare the statistical parameters of the modelled and observed  
 data. Next to that, we calculate the root mean square error (RMSE) and Pearson correlation coefficient across timeseries for  
 each station. Mean and standard deviation of these statistical parameters across all stations provide an indication of the  
 model performance as compared to observations. All values are calculated for both the extended full period (1950-2024) and  
 165 the original dataset (1979-2018) to demonstrate the performance of the model in the backward extension of the dataset.

We also evaluate the effect of the longer record length in the extended dataset on percentiles and return values by comparing  
 values calculated based on the model results for the extended full period (1950-2024) against the period of the original  
 dataset (1979-2018). This comparison shows how the extra 33 years of data alter the results of extreme value analysis.



### 170 3 Data records

The timeseries dataset of total water levels and surge heights for all output points for 1950-2024 based on ERA5 reanalysis data are publicly accessible at the Copernicus Climate Change Service Climate Data Store (CDS) (Muis et al., 2025a). This data is made available at several temporal resolutions: 10 minutes, hourly means and daily maxima. The newly added data extends the already available dataset that covered the period 1979-2018. This dataset includes a global selection of coastal and ocean output points (>43000 points, see **Figure 3** for an indication of coverage). The timeseries data of total water levels includes sea level rise (updated yearly), and uses the local mean sea level over 1986-2005 as a vertical reference. Mean sea level fields are available as a separate variable in the dataset, which could be used to detrend the total water levels .

The descriptive statistics of still water levels (percentiles and extreme values) derived from the GTSM-ERA5-E dataset for each output point are publicly accessible at the Zenodo repository (Muis et al., 2025b). This includes percentiles (1, 5, 10, 25, 50, 75, 90, 95, 99<sup>th</sup>) and extreme values corresponding to different return periods (1, 2, 5, 10, 25, 50, 75 and 100 years). The extreme values include the best-fit values, 5-95% confidence intervals and descriptors of the extreme value fits (shape, scale and location parameters). The descriptive statistics are calculated over the full period of GTSM-ERA5-E dataset, and are based on detrended timeseries of hourly total water levels, removing the effect of sea level rise.

### 185 4 Technical validation

#### 4.1 Still water level statistics validation

A comparison between the modelled and observed values at 262 observation stations globally is shown in Table 1. The comparison is presented for both the extended dataset and the original dataset. In general, there is a good agreement with the hourly timeseries showing a RMSE of 0.20 m and a Pearson correlations coefficient of 0.90 for both datasets. This comparison demonstrates that the extended dataset has the same level of agreement with observations as the original shorter dataset, with the performance metrics for the timeseries and percentiles showing very small differences. This is also the case for metrics representing the higher water levels, such as the monthly water level maxima. This proves that the backward extension of the ERA5 dataset for the period 1950-1978 is well suited for use in the modelling of global water levels, with resulting data having similar (high) quality to the GTSM-ERA5 dataset that covers the period 1979-2018.

Figure 2 shows the spatial distribution of bias between the GTSM-ERA5-E modelled data and GESLA observation data for two statistical values: the 95<sup>th</sup> percentile and the estimated 100-year extreme values of water levels. While the global coverage of filtered GESLA stations is sparse, the comparison shows that the model performance is good for most stations – mean absolute error for the 95<sup>th</sup> percentile of water levels is 0.12 m (s.d. is 0.16 m). There are several stations where the 95<sup>th</sup> percentile values of water levels are underestimated by more than 0.5 m (dark blue dots in Figure 2, bottom left). Further



investigation of the performance at these stations indicates that this discrepancy is mostly associated with the low accuracy of tidal range representation in the GTSM for stations located deep inside estuaries at complex coastlines – the spatial resolution of the global model and the quality of the bathymetry are not sufficient at these locations to represent the tidal ranges correctly. The 100-year return values are generally underestimated by the model, with mean bias of -0.19 m and mean absolute error of 0.25 m (s.d. is 0.25 m). This is also visible in the mostly negative values for bias in 100-year return values across stations as shown in Figure 2 (bottom right). The general underestimation of extremes is consistent with findings from previous work (Muis et al., 2016; Muis et al., 2020; Dullaart et al., 2020) and can be attributed to the underestimation of extreme winds in ERA5 in combination with the model's resolution. Especially storm surges induced by tropical cyclones, which have steep pressure gradients within a relatively small area, will be impacted by the low model resolution and are likely to be underestimated. Moreover, the sample size of events in a record consisting of only several decades is insufficient for properly estimating water level return values in those regions given the low frequency of occurrence of these extreme events.





**Table 1: Model performance of the GSTM-ERA5-E (1950-2024) and GTSM-ERA5 (1979-2018) datasets with still water levels compared to observation data. The values are presented as mean across stations with standard deviation (in brackets).**

Data	Metric	GSTM-ERA5-E	GTSM-ERA5
<b>Timeseries</b>			
Hourly timeseries	RMSE (m)	0.20 (0.19)	0.20 (0.20)
	Pearson corr. coef.	0.90 (0.11)	0.90 (0.12)
Daily maxima timeseries	RMSE (m)	0.18 (0.17)	0.18 (0.17)
	Pearson corr. coef.	0.85 (0.10)	0.86 (0.10)
Monthly maxima timeseries	RMSE (m)	0.21 (0.21)	0.21 (0.21)
	Pearson corr. coef.	0.73 (0.16)	0.73 (0.16)
<b>Percentiles</b>			
95 <sup>th</sup> percentile	Mean bias (m)	-0.01 (0.20)	-0.01 (0.20)
	MAE (m)	0.12 (0.16)	0.12 (0.16)
	MAPE (%)	14.7 (14.5)	14.9 (14.6)
99 <sup>th</sup> percentile	Mean bias (m)	-0.03 (0.23)	-0.03 (0.23)
	MAE (m)	0.14 (0.19)	0.14 (0.19)
	MAPE (%)	13.5 (12.6)	13.5 (12.7)
<b>Return values</b>			
1 in 10-year return value	Mean bias (m)	-0.13 (0.27)	-0.13 (0.28)
	MAE (m)	0.20 (0.23)	0.20 (0.23)
	MAPE (%)	13.6 (11.2)	13.6 (11.3)
1 in 100-year return value	Mean bias (m)	-0.19 (0.29)	-0.19 (0.30)
	MAE (m)	0.25 (0.25)	0.25 (0.26)
	MAPE (%)	15.2 (12.6)	15.1 (13.0)

215

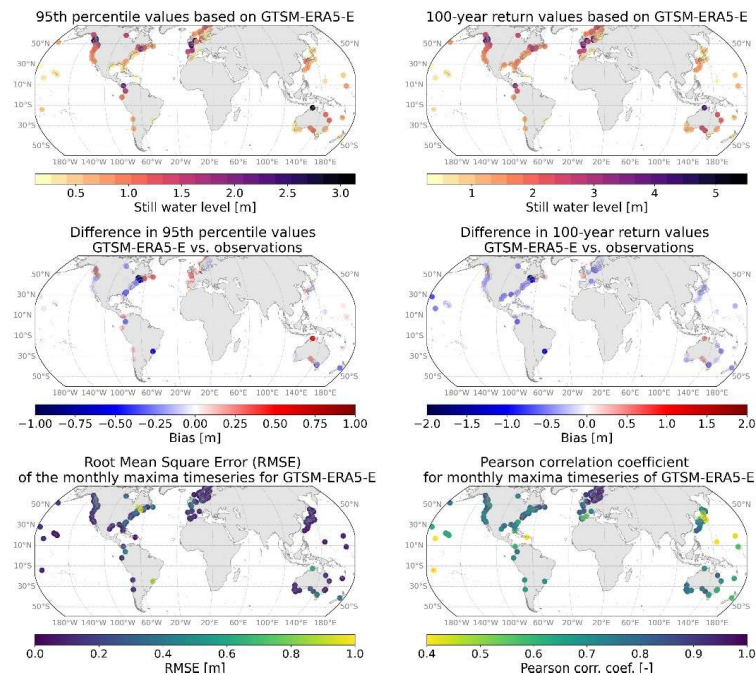


Figure 2: Global map showing the water levels and the bias between modelled and observed water levels. The upper panels show the 95th percentile and the 1 in 100-year extreme return value. The middle panels show the corresponding maps of absolute bias compared to GESLA observations. The lower panels show the RMSE and Pearson correlation coefficient values for GTSM-ERA5-E as compared against observations focusing on the monthly maxima of water levels.

#### 4.2 Impact of dataset extension on water level statistics and extreme return values

The water level statistics derived from the extended GTSM-ERA5-E dataset are compared to those derived from the original GTSM-ERA5 dataset to understand the impact and potential benefits of the longer timeseries. First, we compare the 95<sup>th</sup> percentile values of water levels between 30-year timeseries at the start of the backward extension (1950-1979) to the more recent 30-year period (1990-2019). This comparison shows only minor differences between the two modelled periods, up to several centimetres (see Figure 3, left).

Second, we compare the 100-year return values. The impact of dataset extension on the estimated extreme return values can be seen in Figure 3 (right), where the same extreme value analysis methodology was applied to both datasets. Differences are generally within 0.2 m, although increases and decreases up to 0.5 m occur. The largest increases in the 100-year return values are seen in regions affected by tropical cyclones. This could be linked to the occurrence of tropical cyclones that have



relatively low probabilities and that are most likely under-sampled when a shorter period is considered. This includes regions  
such as Mozambique, Philippines, Caribbean, and northern Australia. There are also regions where there is a decrease, such  
as Northern Europe and parts of the northern coast of the United States. It is known that even within relatively large  
timescales of 60-70 years there can be significant variability in storm surge extremes (Calafat et al., 2022). Future research  
could investigate these trends in detail and quantify the influence of interannual variability as well as climate change.

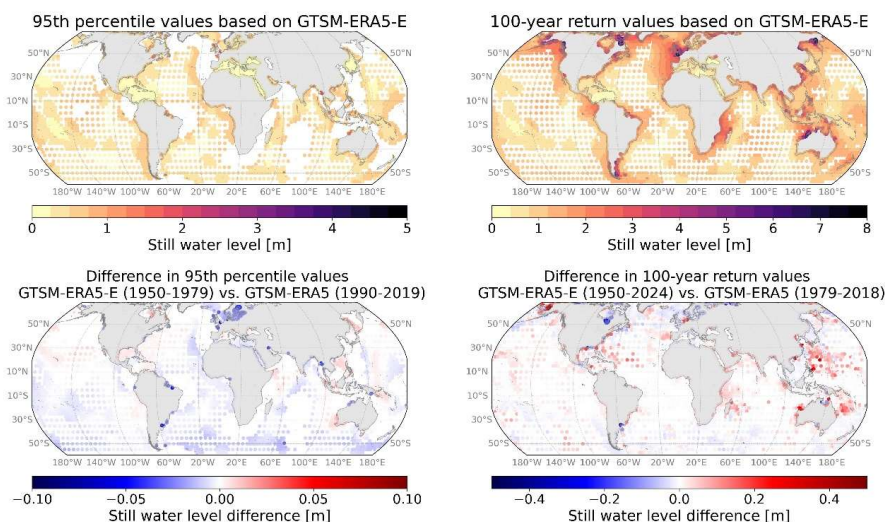
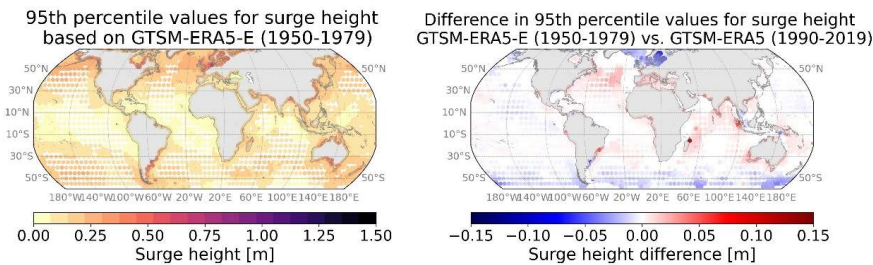


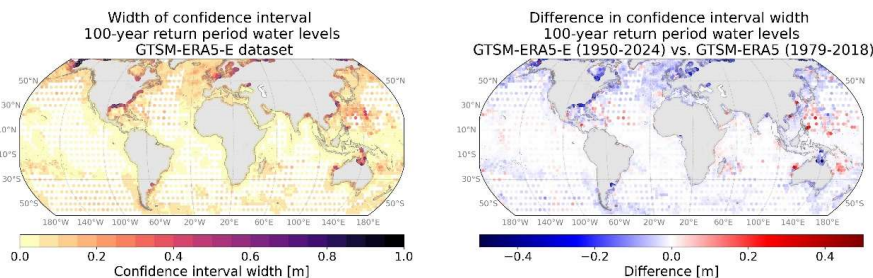
**Figure 3:** Global maps showing the difference in 95<sup>th</sup> percentile values (left) and 100-year return values (right) of total still water levels calculated based on the GTSM-ERA5-E dataset (1950-2024) and the original GTSM-ERA5 dataset (1979-2018). The difference plots are calculated by subtracting the GTSM-ERA5 water levels from the GTSM-ERA5-E water levels.

Surge height statistics are similarly compared by calculating the 99<sup>th</sup> percentile values based the 30-year timeseries at the start of the backward extension (1950-1979) and based on the more recent 30-year period (1990-2019). The difference is shown in **Figure 4**, where it can be seen that in by far the most areas the difference is minor (within 0.05 m), but there are several areas where larger differences are visible. In general, there are negative differences in high-latitude regions, such as Antarctica and Northern Europe, and positive differences difference for most of the rest of the globe. It is not clear what drives these differences in surge statistics and further research could investigate the source.



250 **Figure 4: Global maps showing the difference in 95<sup>th</sup> percentile values for surge height calculated based on a 30-year period at the start of the GTSM-ERA5-E backward extension dataset (1950-1979) and the more recent 30-year period in the original GTSM-ERA5 dataset (1990-2019).**

For 85% of all timeseries data output locations in the dataset the width of the 5-95% confidence intervals for extreme return values of total water levels decreases when the full length of GTSM-ERA5-E dataset is considered in the extreme value analysis. The width of the confidence interval corresponding to the 100-year return values is reduced by 13% on average across all points. **Figure 5** shows the difference in confidence interval width for the 100-year return values, demonstrating that for most regions globally the confidence intervals become narrower. On the other hand, an increase in the width of the confidence intervals is observed at clusters of locations in tropical cyclone regions. This is expected, considering that the sample size for those regions is too small, even with the ERA5-E dataset.



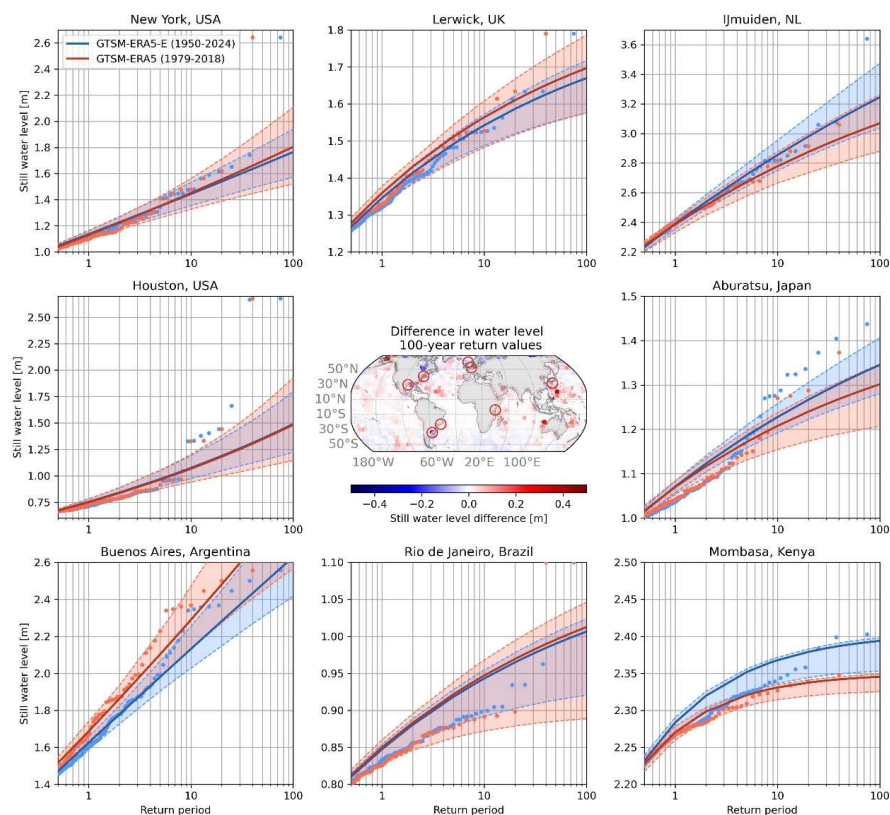
260 **Figure 5 Overview of differences in confidence intervals between the 100-year return values of water levels derived from GTSM-ERA5-E and GTSM-ERA5 datasets.**

Additional insight into the differences between GTSM-ERA5 and GTSM-ERA5-E is obtained by considering the extreme value analysis results for individual locations. **Figure 6** shows return value plots for eight locations globally, including the best-estimate values and confidence intervals. It shows that the effect of using longer records can differ from station to station. At some locations, such as the output locations in the vicinity of New York, Houston and Rio de Janeiro, the best-estimate return values remain practically the same when the longer dataset is considered. However, due to the longer record length the confidence interval becomes narrower. At other locations, such as Buenos Aires and Lerwick, using the longer



dataset yields both lower best-estimate return values and narrower confidence intervals. Yet at some other locations, such as IJmuiden, Aburatsu and Mombasa, higher extreme return values are obtained – at these locations the use of longer timeseries  
270 allowed to include severe storm events beyond the temporal scope of the original 1979-2018 dataset, suggesting higher long-term extremes than initially estimated using the shorter dataset. This overview highlights the range of possible changes in estimated extreme water levels that can result from using a dataset covering a longer period of time. While for most (seven out of the eight) locations shown here, the return periods based on GTSM-ERA5-E are still within the confidence bounds of those based on GTSM-ERA5, the difference for higher return periods can be considerable. Hence, the plots indicate that in  
275 both tropical and extra-tropical regions the length of 40-years of data (as in GTSM-ERA5) may not always be sufficient to robustly estimate return periods.

It must be noted that the quality of the extreme value analysis fits based on the peak-over-threshold method with fixed threshold selection varies from location to location. In the examples illustrated in **Figure 6** it can be seen that at some  
280 locations the present single-distribution approach is not sufficient to accurately estimate the extreme return values, this is the case for Houston and Aburatsu, where the higher extremes are affected by tropical cyclones. In other cases, for example in Mombasa, the water levels are largely tide-driven with very small differences between the extreme return values.



285 **Figure 6: Extreme value analysis return value plots for multiple coastal locations globally demonstrating the difference between extremes estimated based on the GTSM-ERA5-E dataset (1950-2024) and shorter GTSM-ERA5 dataset (1979-2018). The shaded areas indicate the 5-95% confidence intervals.**

#### 4.3 Dataset performance in representing individual storm events

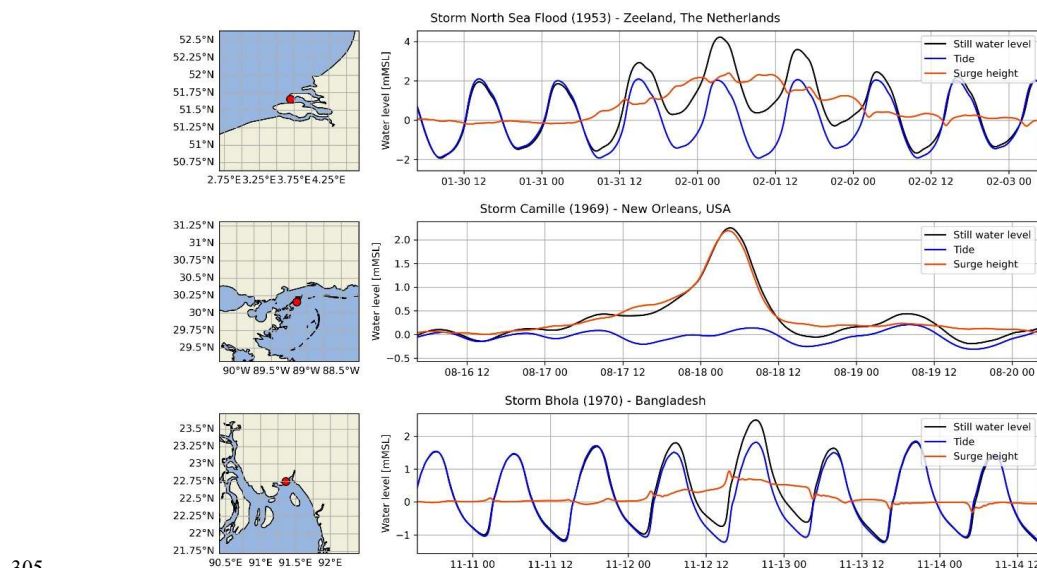
In addition to the impact of the dataset extension on water level statistics and extreme return values, we also demonstrate the water level data corresponding to individual major storms in the timeline covered by the extended dataset. This includes the storm surge caused by the extratropical storm in the North Sea in 1953, tropical cyclone Camille (1969) that impacted the United States, and Bhola (1970) tropical cyclone that impacted present-day Bangladesh. **Figure 7** shows the timeseries of total water level and storm surge for these storm events at the impacted locations. In the case of the North Sea storm in 1953, the maximum surge was 2.5 m, which is in full agreement with observations (Gerritsen, 2005). For Camille (1969) we find a maximum water level of 2.2 m that mainly consists of surge, which is significantly lower than the reported values of 5-6 m





295 (NOAA, 1972). For Bhola we also find significantly underestimated values with a maximum surge of 1 m, which is much lower than reported values of over 6 m (Frank and Husain, 1971).

There is considerable uncertainty associated with the reported storm surges (e.g. whether the reported values include tides and waves, unknown location of observations and their vertical reference), however the severe underestimation of GTSM-  
 300 ERA5 for these events is evident. This can be the result of the combination of the poor representation of very intense tropical cyclone events in ERA5; and the relatively coarse spatial resolution of GTSM (approximately 2.5 km), which is insufficient to represent complex areas. These findings are consistent with results from previous studies (Dullaart et al., 2020; Muis et al., 2019; Ikeuchi et al., 2017), in which we concluded that while GTSM shows good performance in general, there can be severe underestimation of tropical-cyclone induced storm surge.



305 **Figure 7: Water levels, tides and surge heights extracted from the GTSM-ERA5-E database for locations affected by high surges during historical storm events, including the winter storm in the North Sea in 1953 and tropical storms Camille (1969) and Bhola (1970).**

### Data availability

310 The dataset of total water levels and surge height timeseries described in this manuscript can be accessed at the Copernicus Climate Change Service Climate Data Store under DOI 10.24381/cds.a6d42d60 (Muis et al., 2025a). The descriptive statistics of total water levels (percentiles and extreme values) derived from the timeseries dataset can be accessed at Zenodo under DOI 10.5281/zenodo.14671593 (Muis et al., 2025b).



### Code availability

315 The Delft3D Flexible Mesh software that was used for the hydrodynamic modelling is openly available for download at <https://download.deltares.nl/en/download/delft3d-fm/>. A singularity container was used to run in a high-performance computing environment: <https://oss.deltares.nl/web/delft3dfm/get-started>. All code (Python and bash scripts) that was used to generate the datasets described here are publicly available via GitHub and preserved at Zenodo under DOI 10.5281/zenodo.14671593 (Muis et al., 2025b).

### 320 Conclusions

This paper presents an extended dataset of oceanic and coastal water levels and surge heights globally, derived using the ERA5 reanalysis from 1950 to the present. This dataset is methodologically consistent with the previous version of the dataset covering time period of 1979 to 2018. The extended dataset spans a period of 75 years, offering the basis for deriving long-term statistics and extremes, as well as analysing specific past events. An accompanying dataset of water level statistics globally is presented in this paper. The accuracy of the dataset is analysed through statistical validation against a global dataset of water level observations (GESLA) and through the more detailed look at three individual past severe storm events covered by the dataset extension.

There are several aspects of the presented dataset that are advised to consider when using this dataset. While the dataset offers significant extension of the temporal coverage, caution is advised when using the ERA5-based dataset to derive water level statistics in areas prone to tropical cyclones, because the record length of 75 years can be still insufficient to account for low-probability events (Lin and Emanuel, 2015). Next to that, it is important to keep in mind the limitations of a global dataset. First, it is well-reported in literature that the intensity of extreme storms and tropical cyclones in particular will be underestimated in ERA5 (Dulac et al., 2024), which will also underestimate storm surge levels (Bloemendaal et al., 2019). Second, as a global model, GTSM does not capture local storm surges in very complex coastal areas, the observed surges can be found to be much higher than modelled values. Also the low accuracy of global bathymetry data may negatively affect the accuracy of our results. Therefore, we recommend that if users want to use the global data for a regional study, they need to consider the specific context and evaluate the suitability of the modelling assumptions.

340 When it comes to the provided extreme value statistics of total water levels, this data is intended for first-order global overview of extremes. Extreme value analysis performed at a global scale using fixed thresholds carries considerable uncertainty. In local studies on water level and surge extremes it is strongly recommended to perform more accurate extreme value analysis based on the available water level and surge timeseries, where individual fits can be evaluated and adjusted by setting appropriate thresholds.

345





The dataset provides a valuable resource for assessing flood risks in coastal regions. The time series data can be used as input for flood models to investigate historical events, while the extreme return values can inform flood risk assessments (Tiggeloven et al., 2020; Lincke and Hinkel, 2018). In wave-dominated regions, we recommend to combine the GTSM-derived water levels with wave setup computed based on the ERA5 wave reanalysis (Kirezci et al., 2020). We also  
350 acknowledge that in some cases the sea level reanalysis can be improved by combining it with mean sea level reconstructions (Treu et al., 2023) that account for ocean processes that are not resolved by GTSM. For regional to local-scale application both statistical and dynamic downscaling could be explored.

#### Author contribution

All authors contributed to code development. S.M. drafted the initial version of the manuscript. Data analysis and validation  
355 of data were carried out by N.A. under supervision of S.M.

#### Competing interests

The authors declare that they have no conflict of interest.

#### Acknowledgements

The research leading to these results received funding from the Deltares Strategic Research Program. S.M. received  
360 additional funding from the CHANCE research program, which is financed by the Dutch Research Council (NWO) under the grant OCENW.M.21.109. We thank SURF ([www.surf.nl](http://www.surf.nl)) for the support in using the National Supercomputer Snellius. We also thank Dr. José A. A. Antolínez (TU Delft) for discussions that helped in this research, Robyn Gwee (National University of Singapore) for sharing examples of prior GTSM data processing that was developed further in this work, and Dr. Kun Yan (Deltares) for support in making the data available through the C3S Climate Data Store.

#### 365 References

- Arns, A., Wahl, T., Wolff, C., Vafeidis, A. T., Haigh, I. D., Woodworth, P., Niehüser, S., and Jensen, J.: Non-linear interaction modulates global extreme sea levels, coastal flood exposure, and impacts, *Nat Commun*, 11, 1918, <https://doi.org/10.1038/s41467-020-15752-5>, 2020.
- Bell, B., Hersbach, H., Simmons, A., Berrisford, P., Dahlgren, P., Horányi, A., Muñoz-Sabater, J., Nicolas, J., Radu, R.,  
370 Schepers, D., Soci, C., Villaume, S., Bidlot, J., Haimberger, L., Woollen, J., Buontempo, C., and Thépaut, J.: The ERA5 global reanalysis: Preliminary extension to 1950, *Quart J Royal Meteor Soc*, 147, 4186–4227, <https://doi.org/10.1002/qj.4174>, 2021.



- Bloemendaal, N., Muis, S., Haarsma, R. J., Verlaan, M., Irazoqui Apecechea, M., De Moel, H., Ward, P. J., and Aerts, J. C. J. H.: Global modeling of tropical cyclone storm surges using high-resolution forecasts, *Clim Dyn*, 52, 5031–5044, <https://doi.org/10.1007/s00382-018-4430-x>, 2019.
- Bocharov, G.: *pyextremes*, 2023.
- Brown, S., Nicholls, R., Goodwin, P., Haigh, I., Lincke, D., Vafeidis, A., and Hinkel, J.: Quantifying Land and People Exposed to Sea-Level Rise with No Mitigation and 1.5°C and 2.0°C Rise in Global Temperatures to Year 2300, *Earth's Future*, 6, <https://doi.org/10.1002/2017ef000738>, 2018.
- Calafat, F. M., Wahl, T., Tadesse, M. G., and Sparrow, S. N.: Trends in Europe storm surge extremes match the rate of sea-level rise, *Nature*, 603, 841–845, <https://doi.org/10.1038/s41586-022-04426-5>, 2022.
- Camus, P., Haigh, I., Nasr, A., Wahl, T., Darby, S., and Nicholls, R.: Regional analysis of multivariate compound flooding potential: sensitivity analysis and spatial patterns, <https://doi.org/10.5194/nhess-2021-50>, 2021.
- Carrère, L., Lyard, F., Cancet, M., Guillot, A., and Roblou, L.: FES 2012: a new global tidal model taking advantage of nearly 20 years of altimetry, in: *20 Years of Progress in Radar Altimetry*, Venice, Italy, 2012.
- Charnock, H.: Wind stress on a water surface, *Quart J Royal Meteor Soc*, 81, 639–640, <https://doi.org/10.1002/qj.49708135027>, 1955.
- Couasnon, A., Eilander, D., Muis, S., Veldkamp, T. I. E., Haigh, I. D., Wahl, T., Winsemius, H. C., and Ward, P.: Measuring compound flood potential from river discharge and storm surge extremes at the global scale, *Natural Hazards and Earth System Sciences*, 20, 489–504, <https://doi.org/10.5194/nhess-20-489-2020>, 2020.
- Dulac, W., Cattiaux, J., Chauvin, F., Bourdin, S., and Fromang, S.: Assessing the representation of tropical cyclones in ERA5 with the CNRM tracker, *Clim Dyn*, 62, 223–238, <https://doi.org/10.1007/s00382-023-06902-8>, 2024.
- Dullaart, J. C. M., Muis, S., Bloemendaal, N., and Aerts, J. C. J. H.: Advancing global storm surge modelling using the new ERA5 climate reanalysis, *Clim Dyn*, 54, 1007–1021, <https://doi.org/10.1007/s00382-019-05044-0>, 2020.
- Dullaart, J. C. M., Muis, S., Bloemendaal, N., Chertova, M. V., Couasnon, A., and Aerts, J. C. J. H.: Accounting for tropical cyclones more than doubles the global population exposed to low-probability coastal flooding, *Commun Earth Environ*, 2, 1–11, <https://doi.org/10.1038/s43247-021-00204-9>, 2021.
- Eilander, D., Couasnon, A., Ikeuchi, H., Muis, S., Yamazaki, D., Winsemius, H. C., and Ward, P. J.: The effect of surge on riverine flood hazard and impact in deltas globally, *Environ. Res. Lett.*, 15, 104007, <https://doi.org/10.1088/1748-9326/ab8ca6>, 2020.
- EMODnet Bathymetry Consortium: EMODnet Digital Bathymetry (DTM 2018), <https://doi.org/10.12770/18FF0D48-B203-4A65-94A9-5FD8B0EC35F6>, 2018.
- Enríquez, A. R., Wahl, T., Marcos, M., and Haigh, I. D.: Spatial Footprints of Storm Surges Along the Global Coastlines, *JGR Oceans*, 125, e2020JC016367, <https://doi.org/10.1029/2020JC016367>, 2020.
- Fang, J., Sun, S., Shi, P., and Wang, J.: Assessment and Mapping of Potential Storm Surge Impacts on Global Population and Economy, *Int J Disaster Risk Sci*, 5, 323–331, <https://doi.org/10.1007/s13753-014-0035-0>, 2014.



- Frank, N. L. and Husain, S. A.: The Deadliest Tropical Cyclone in History, *Bull. Amer. Meteor. Soc.*, 52, 438–445, [https://doi.org/10.1175/1520-0477\(1971\)052<0438:TDTCIH>2.0.CO;2](https://doi.org/10.1175/1520-0477(1971)052<0438:TDTCIH>2.0.CO;2), 1971.
- Fretwell, P., Pritchard, H. D., Vaughan, D. G., Bamber, J. L., Barrand, N. E., Bell, R., Bianchi, C., Bingham, R. G.,  
 410 Blankenship, D. D., Casassa, G., Catania, G., Callens, D., Conway, H., Cook, A. J., Corr, H. F. J., Damaske, D., Damm, V.,  
 Ferraccioli, F., Forsberg, R., Fujita, S., Gim, Y., Gogineni, P., Griggs, J. A., Hindmarsh, R. C. A., Holmlund, P., Holt, J. W.,  
 Jacobel, R. W., Jenkins, A., Jokat, W., Jordan, T., King, E. C., Kohler, J., Krabill, W., Riger-Kusk, M., Langley, K. A.,  
 Leitchenkov, G., Leuschen, C., Luyendyk, B. P., Matsuoka, K., Mouginot, J., Nitsche, F. O., Nogi, Y., Nost, O. A., Popov,  
 S. V., Rignot, E., Rippin, D. M., Rivera, A., Roberts, J., Ross, N., Siegert, M. J., Smith, A. M., Steinhage, D., Studinger, M.,  
 415 Sun, B., Tinto, B. K., Welch, B. C., Wilson, D., Young, D. A., Xiangbin, C., and Zirizzotti, A.: Bedmap2: improved ice bed,  
 surface and thickness datasets for Antarctica, *The Cryosphere*, 7, 375–393, <https://doi.org/10.5194/tc-7-375-2013>, 2013.
- GEBCO: General Bathymetric Chart of the Oceans (GEBCO). 2014 grid., 2014.
- Gerritsen, H.: What happened in 1953? The Big Flood in the Netherlands in retrospect, *Phil. Trans. R. Soc. A.*, 363, 1271–  
 1291, <https://doi.org/10.1098/rsta.2005.1568>, 2005.
- 420 Ghanavati, M., Young, I., Kirezci, E., Ranasinghe, R., Duong, T. M., and Luijendijk, A. P.: An assessment of whether long-  
 term global changes in waves and storm surges have impacted global coastlines, *Sci Rep*, 13, 11549,  
<https://doi.org/10.1038/s41598-023-38729-y>, 2023.
- Haigh, I. D., Marcos, M., Talke, S. A., Woodworth, P. L., Hunter, J. R., Hague, B. S., Arns, A., Bradshaw, E., and  
 Thompson, P.: GESLA Version 3: A major update to the global higher-frequency sea-level dataset, *Geoscience Data Journal*,  
 425 10, 293–314, <https://doi.org/10.1002/gdj3.174>, 2023.
- Hersbach, H., Bell, B., Berrisford, P., Biavati, G., Horanyi, A., Muñoz Sabater, J., Nicolas, J., Peubey, C., Radu, R., Rozum,  
 I., Schepers, D., Simmons, A., Soci, C., Dee, D., and Thepaut, J.-N.: ERA5 hourly data on single levels from 1940 to  
 present, <https://doi.org/10.24381/CDS.ADBB2D47>, 2023.
- Hinkel, J., Lincke, D., Vafeidis, A., Perrette, M., Nicholls, R., Tol, R., Marzeion, B., Fettweis, X., Ionescu, C., and  
 430 Levermann, A.: Coastal flood damage and adaptation cost under 21st century sea-level rise, *Proceedings of the National  
 Academy of Sciences of the United States of America*, 111, 3292–7, <https://doi.org/10.1073/pnas.1222469111>, 2014.
- Hinkel, J., Feyen, L., Hemer, M., Le Cozannet, G., Lincke, D., Marcos, M., Mentaschi, L., Merken, J., Moel, H., Muis, S.,  
 Nicholls, R., Vafeidis, A., Wal, R. S. W., Voudoukas, M., Wahl, T., Ward, P., and Wolff, C.: Uncertainty and Bias in  
 Global to Regional Scale Assessments of Current and Future Coastal Flood Risk, *Earth's Future*, 9,  
 435 <https://doi.org/10.1029/2020EF001882>, 2021.
- Hoyer, S. and Hamman, J.: xarray: N-D labeled Arrays and Datasets in Python, *Journal of Open Research Software*, 5,  
<https://doi.org/10.5334/jors.148>, 2017.
- Ikeuchi, H., Hirabayashi, Y., Yamazaki, D., Muis, S., Ward, P. J., Winsemius, H. C., Verlaan, M., and Kanae, S.: Compound  
 simulation of fluvial floods and storm surges in a global coupled river-coast flood model: Model development and its



- 440 application to 2007 Cyclone Sidr in Bangladesh, *J Adv Model Earth Syst*, 9, 1847–1862,  
<https://doi.org/10.1002/2017MS000943>, 2017.
- IPCC: Climate Change 2013: The Physical Science Basis. Contribution of Working Group I to the Fifth Assessment Report of the Intergovernmental Panel on Climate Change, edited by: Stocker, T. F., Qin, G.-K., Plattner, M., Tignor, S. K., Allen, J., Boschung, A., Nauels, Y., Xia, V., Bex, and P.M. Midgley. Cambridge University Press, Cambridge, United Kingdom, 2013.
- 445 Kernkamp, H. W. J., Van Dam, A., Stelling, G. S., and De Goede, E. D.: Efficient scheme for the shallow water equations on unstructured grids with application to the Continental Shelf, *Ocean Dynamics*, 61, 1175–1188,  
<https://doi.org/10.1007/s10236-011-0423-6>, 2011.
- Kirezci, E., Young, I. R., Ranasinghe, R., Muis, S., Nicholls, R. J., Lincke, D., and Hinkel, J.: Projections of global-scale extreme sea levels and resulting episodic coastal flooding over the 21st Century, *Sci Rep*, 10, 11629,  
 450 <https://doi.org/10.1038/s41598-020-67736-6>, 2020.
- Koks, E. E., Le Bars, D., Essenfelder, A. H., Nirandjan, S., and Sayers, P.: The impacts of coastal flooding and sea level rise on critical infrastructure: a novel storyline approach, *Sustainable and Resilient Infrastructure*, 8, 237–261,  
<https://doi.org/10.1080/23789689.2022.2142741>, 2023.
- Le Bars, D.: Uncertainty in Sea Level Rise Projections Due to the Dependence Between Contributors, *Earth’s Future*, 6,  
 455 1275–1291, <https://doi.org/10.1029/2018EF000849>, 2018.
- Li, H., Haer, T., Couasnon, A., Enríquez, A. R., Muis, S., and Ward, P. J.: A spatially-dependent synthetic global dataset of extreme sea level events, *Weather and Climate Extremes*, 41, 100596, <https://doi.org/10.1016/j.wace.2023.100596>, 2023.
- Lin, N. and Emanuel, K.: Grey swan tropical cyclones, *Nature Clim Change*, 6, 106–111,  
<https://doi.org/10.1038/nclimate2777>, 2016.
- 460 Lincke, D. and Hinkel, J.: Economically robust protection against 21st century sea-level rise, *Global Environmental Change*, 51, 67–73, <https://doi.org/10.1016/j.gloenvcha.2018.05.003>, 2018.
- Menéndez, M. and Woodworth, P. L.: Changes in extreme high water levels based on a quasi-global tide-gauge data set, *J. Geophys. Res.*, 115, 2009JC005997, <https://doi.org/10.1029/2009JC005997>, 2010.
- Muis, S., Verlaan, M., Winsemius, H. C., Aerts, J. C. J. H., and Ward, P. J.: A global reanalysis of storm surges and extreme  
 465 sea levels, *Nat Commun*, 7, 11969, <https://doi.org/10.1038/ncomms11969>, 2016.
- Muis, S., Verlaan, M., Nicholls, R., Brown, S., Hinkel, J., Lincke, D., Vafeidis, A., Scussolini, P., Winsemius, H., and Ward, P.: A comparison of two global datasets of extreme sea levels and resulting flood exposure, *Earth’s Future*, 5,  
<https://doi.org/10.1002/2016EF000430>, 2017.
- Muis, S., Haigh, I. D., Guimarães Nobre, G., Aerts, J. C. J. H., and Ward, P. J.: Influence of El Niño–Southern Oscillation on  
 470 Global Coastal Flooding, *Earth’s Future*, 6, 1311–1322, <https://doi.org/10.1029/2018EF000909>, 2018.
- Muis, S., Lin, N., Verlaan, M., Winsemius, H. C., Ward, P. J., and Aerts, J. C. J. H.: Spatiotemporal patterns of extreme sea levels along the western North-Atlantic coasts, *Sci Rep*, 9, 3391, <https://doi.org/10.1038/s41598-019-40157-w>, 2019.



- Muis, S., Irazoqui, M., Dullaart, J., Rego, J., Madsen, K., Su, J., Yan, K., and Verlaan, M.: A High-Resolution Global Dataset of Extreme Sea Levels, Tides, and Storm Surges, Including Future Projections, *Frontiers in Marine Science*, 7, 263, <https://doi.org/10.3389/fmars.2020.00263>, 2020.
- Muis, S., Aerts, J. C. J. H., Á. Antolínez, J. A., Dullaart, J. C., Duong, T. M., Erikson, L., Haarsma, R. J., Apecechea, M. I., Mengel, M., Le Bars, D., O'Neill, A., Ranasinghe, R., Roberts, M. J., Verlaan, M., Ward, P. J., and Yan, K.: Global Projections of Storm Surges Using High-Resolution CMIP6 Climate Models, *Earth's Future*, 11, e2023EF003479, <https://doi.org/10.1029/2023EF003479>, 2023a.
- Muis, S., Irazoqui Apecechea, M., and Bars, D. L.: Mean sea level fields used within the GTSMip simulations, <https://doi.org/10.5281/ZENODO.3948088>, 2023b.
- Muis, S., Irazoqui Apecechea, M., Antolinez, J. A. Á., Verlaan, M., Yan, K., Dullaart, J., Aerts, J. C. J. H., Duong, T., Ranasinghe, R., Le Bars, D., Haarsma, R. J., and Roberts, M.: Global sea level change time series from 1950 to 2050 derived from reanalysis and high resolution CMIP6 climate projections, <https://doi.org/10.24381/CDS.A6D42D60>, 2025a.
- Muis, S., Aleksandrova, N., Veenstra, J., and Gwee, R.: GTSM-ERA5-E dataset - Data underlying the paper “Global dataset of storm surges and extreme sea levels for 1950-2024 based on the ERA5 climate reanalysis,” <https://doi.org/10.5281/ZENODO.14671593>, 2025b.
- Nasr, A., Wahl, T., Rashid, M. M., Camus, P., and Haigh, I. D.: Assessing the dependence structure between oceanographic, fluvial, and pluvial flooding drivers along the United States coastline, *Hydrology and Earth System Sciences*, 25, 6203–6222, <https://doi.org/10.5194/hess-25-6203-2021>, 2021.
- Hurricane Camille 1969: <https://www.weather.gov/lch/1969Camille-Surge>, last access: 5 August 2025.
- Reimann, L., Vafeidis, A. T., Brown, S., Hinkel, J., and Tol, R. S. J.: Mediterranean UNESCO World Heritage at risk from coastal flooding and erosion due to sea-level rise, *Nat Commun*, 9, 4161, <https://doi.org/10.1038/s41467-018-06645-9>, 2018.
- Ridder, N. N., Pitman, A. J., Westra, S., Ukkola, A., Do, H. X., Bador, M., Hirsch, A. L., Evans, J. P., Di Luca, A., and Zscheischler, J.: Global hotspots for the occurrence of compound events, *Nat Commun*, 11, 5956, <https://doi.org/10.1038/s41467-020-19639-3>, 2020.
- Stolte, W., Baart, F., Muis, S., Hijma, M., Taal, M., Le Bars, D., and Drijfhout: Zeespiegelmonitor 2022., 2023.
- Tadesse, M. G., Wahl, T., Rashid, M. M., Dangendorf, S., Rodríguez-Enríquez, A., and Talke, S. A.: Long-term trends in storm surge climate derived from an ensemble of global surge reconstructions, *Sci Rep*, 12, 13307, <https://doi.org/10.1038/s41598-022-17099-x>, 2022.
- Tiggeloven, T., De Moel, H., Winsemius, H. C., Eilander, D., Erkens, G., Gebremedhin, E., Diaz Loaiza, A., Kuzma, S., Luo, T., Iceland, C., Bouwman, A., Van Huijstee, J., Ligtoet, W., and Ward, P. J.: Global-scale benefit–cost analysis of coastal flood adaptation to different flood risk drivers using structural measures, *Nat. Hazards Earth Syst. Sci.*, 20, 1025–1044, <https://doi.org/10.5194/nhess-20-1025-2020>, 2020.



- 505 Treu, S., Muis, S., Dangendorf, S., Wahl, T., Oelsmann, J., Heinicke, S., Frieler, K., and Mengel, M.: Reconstruction of hourly coastal water levels and counterfactuals without sea level rise for impact attribution, <https://doi.org/10.5194/essd-2023-112>, 2023.
- Verschuur, J., Koks, E. E., Li, S., and Hall, J. W.: Multi-hazard risk to global port infrastructure and resulting trade and logistics losses, *Commun Earth Environ*, 4, 5, <https://doi.org/10.1038/s43247-022-00656-7>, 2023.
- 510 Wahl, T., Haigh, I. D., Nicholls, R. J., Arns, A., Dangendorf, S., Hinkel, J., and Slangen, A. B. A.: Understanding extreme sea levels for broad-scale coastal impact and adaptation analysis, *Nat Commun*, 8, 16075, <https://doi.org/10.1038/ncomms16075>, 2017.
- Woodworth, P. L., Melet, A., Marcos, M., Ray, R. D., Wöppelmann, G., Sasaki, Y. N., Cirano, M., Hibbert, A., Huthnance, J. M., Monserrat, S., and Merrifield, M. A.: Forcing Factors Affecting Sea Level Changes at the Coast, *Surv Geophys*, 40, 1351–1397, <https://doi.org/10.1007/s10712-019-09531-1>, 2019.
- 515